Synthesis and Photoelectrochemical Behavior of Nitrogen-doped $NaTaO_3$

Xuewen Wang,[1] Gang Liu,[1,2] Zhi-Gang Chen,[1] Feng Li,[1] Gao Qing Lu,*[2] and Hui-Ming Cheng*[1]
[1]*Shenyang National Laboratory for Materials Science, Institute of Metal Research, Chinese Academy of Sciences, 72 Wenhua Road, Shenyang 110016, P. R. China*
[2]*ARC Centre of Excellence for Functional Nanomaterials, School of Engineering and Australian Institute of Bioengineering and Nanotechnology, The University of Queensland, Qld. 4072, Australia*

(Received November 20, 2008; CL-081098; E-mail: maxlu@uq.edu.au, cheng@imr.ac.cn)

Well-dispersed $NaTaO_3$ particles with a cubic morphology and high crystallinity were prepared by a hydrothermal route. The $NaTaO_3$ was doped with nitrogen by heat treatment in ammonia atmosphere. The nitrogen-doped $NaTaO_3$ shows an additional visible light absorption shoulder up to 550 nm. The photoelectrochemical investigation demonstrated that the photocurrent density of the photoanode of the nitrogen-doped $NaTaO_3$ was enhanced under the irradiation of both UV–visible light and visible light, compared to that of the undoped $NaTaO_3$.

Recently, more and more efforts[1–3] have been devoted to developing visible-light-responsive photocatalysts. Among the many photocatalysts discovered to date, $NaTaO_3$ shows high photoactivity. However, the band gap of $NaTaO_3$ is ca. 4.0 eV and does not exhibit visible light absorption. Doping is considered to be an effective route to improve the photocatalytic performance of photocatalysts.[4,5] Nitrogen doping, especially in titania-based photocatalysts,[6,7] has been extensively investigated, and many routes have been explored.[8–11] Among these routes, the most simple and facile one is thermal treatment in ammonia atmosphere, especially for multicomponent compounds derived via traditional solid-state reactions. The advantage of this route lies in that heating can supply enough energy for incorporating N atoms, which is essential for the realization of nitrogen doping in multicomponent compounds with a large crystal size and high crystallinity. So far, nitrogen doping has been applied to many multicomponent systems, such as $ATaO_2N$ (A = Ba, Sr, and Ca) and $LaTaON_2$.[12,13] However, nitrogen doping has rarely been realized in $NaTaO_3$ systems, which is the most efficient for photoelectrochemical splitting of pure water to hydrogen under UV irradiation,[14] because $NaTaO_3$ obtained from solid-state reactions is easily transformed to Ta_3N_5.

In this study, we report nitrogen-doped $NaTaO_3$ by heat treatment of hydrothermally synthesized cubic $NaTaO_3$ in ammonia atmosphere. After nitrogen doping, the crystal structure of $NaTaO_3$ is well retained, but the band gap of $NaTaO_3$ decreases from ca. 4.0 to 3.7 eV. Furthermore, an additional visible light absorption in the photon energy up to ca. 2.25 eV is introduced. Compared to the undoped $NaTaO_3$, the nitrogen-doped $NaTaO_3$ photoanode is more active under the irradiation of visible light in photoelectrochemical processes.

For $NaTaO_3$ preparation, 0.2 mol of $TaCl_5$ (99.99%, Alfa Aesar) was dissolved in 10 mL of 7 M HCl solution. Diluted ammonia was slowly added dropwise into the hydrochloric acid solution of $TaCl_5$ to neutralize it for the hydrolysis of $TaCl_5$ (pH 7). The precipitate obtained was added to 60 mL of 2 M NaOH solution to obtain a suspension, and then the suspension was placed into a Teflon autoclave and heated at 140 °C for 20 h.

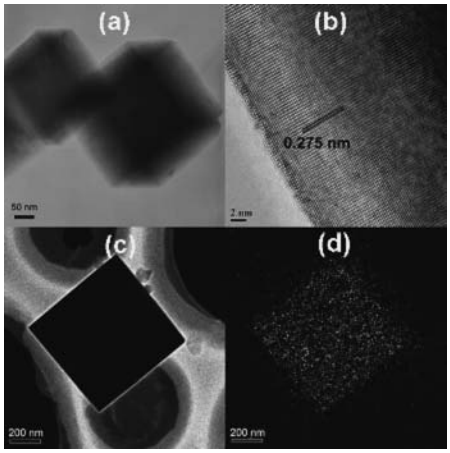

Figure 1. TEM image (a), HRTEM image (b), energy-filtered TEM image (c), and N mapping (d), of the nitrogen-doped $NaTaO_3$.

After washing and drying at 60 °C for 12 h, the undoped $NaTaO_3$ was obtained. Nitrogen-doped $NaTaO_3$ was prepared by heating the $NaTaO_3$ under NH_3 flow of 25 mL·min^{-1} at 850 °C for 4 h.

Compared to the irregular $NaTaO_3$ particles derived from traditional solid-state reaction routes, the $NaTaO_3$ particles we prepared are cubic-shaped with a single crystal structure. After nitrogen doping, XRD patterns of the nitrogen-doped $NaTaO_3$ remain the same as the undoped $NaTaO_3$ (Figure S1),[22] and both crystal structure (Figure S1)[22] and particle morphology (Figure 1a and Figure S2)[22] of the undoped $NaTaO_3$ are well retained. The lattice spacing of 0.275 nm in Figure 1b is consistent with the lattice spacing of the {200} planes of cubic $NaTaO_3$. In contrast to the reported hydrothermal route[15,16] with Ta_2O_5 as precursor, our route has the merit of low concentration of NaOH solution, high dispersion, and pure single phase, which are helpful for nitrogen doping.

Energy-filtered TEM was used to determine the elemental mapping of N in the photocatalyst. Figure 1c shows the general morphology, and Figure 1d is N mapping of the nitrogen-doped $NaTaO_3$. These results show that nitrogen atoms are homogeneously distributed in the nitrogen-doped $NaTaO_3$ particles. XPS results (Figure S3)[22] confirm the existence of the oxidation state of N (395.2 eV) in nitrogen-doped $NaTaO_3$, and the content of N dopant on the surface of the nitrogen-doped $NaTaO_3$ is estimated to be 1.5 atom %.

Compared to the undoped $NaTaO_3$, the band gap of nitrogen-doped $NaTaO_3$ decreases from ca. 4.0 to 3.7 eV (Figure 2). In addition, the absorption edge of $NaTaO_3$ after nitrogen doping is extended to ca. 2.25 eV, which means light absorption extend-

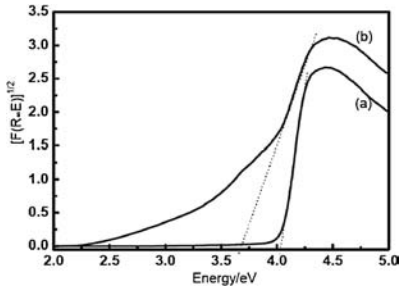

Figure 2. Plots of transformed Kubelka–Munk function vs. the energy of light absorbed of (a) $NaTaO_3$ and (b) nitrogen-doped $NaTaO_3$.

ing to ca. 550 nm. For metal oxide semiconductors,[17,18] the valence bands consist of main O 2p states and partial metal d states. The mechanism for introducing visible light absorption in anion-doped metal oxide semiconductors is either generating localized states of anion dopants or narrowing the band gap by elevating the valence band maximum. In our nitrogen-doped $NaTaO_3$, both mechanisms are involved, and O–Ta–N bonds and N–Ta–N bonds exist. The mixture of N 2p with O 2p states caused by the stronger interaction between Ta and N in N–Ta–N bonds results in the decreased band gap of the nitrogen-doped $NaTaO_3$. Compared to that of N atoms in N–Ta–N bonds, the binding energy of N atoms in O–Ta–N bonds is lower owing to stronger electronegativity of O than N. So the weaker interaction between Ta and N in O–Ta–N bonds gives rise to the localized states with higher energy level in the band gap, which is responsible for the additional shoulder of light absorption in the nitrogen-doped $NaTaO_3$. Moreover, oxygen vacancies, inevitably existing in the nitrogen-doped $NaTaO_3$ system in order to keep the charge balance, give rise to the localized states with higher energy level in the band gap, which is also responsible for the additional shoulder of light absorption.

Photoelectrochemical measurements are widely employed to determine the photoactivity of semiconductor photoanodes.[19–21] Following reported procedures,[20] the ITO photoanode consisting of the nitrogen-doped $NaTaO_3$ shows higher photocurrent than that with $NaTaO_3$ under the irradiation of both UV–visible light (Figure S4)[22] and visible light (Figure 3). It is noted that the enhanced photocurrent is positively dependent on the increase of N dopant in $NaTaO_3$ before the crystal structure is changed. The turn-on potentials of photocurrent for the anodes of the undoped and nitrogen-doped $NaTaO_3$ under the irradiation of visible light are ca. 0.1 and -0.12 V. Generally, the turn-on potential can roughly determine the flat-band potential of the photoanode in a given electrolyte, while the flat-band potential is closely related to the Fermi level of the semiconductor photoanode. For nitrogen-doped $NaTaO_3$, the introduced localized states in the band gap and mixed states of N 2p with valence band can exert a great influence on its Fermi level and hence its flat-band potential and turn-on potential. In this case, oxygen vacancies also contribute to the elevation of Fermi level. Obviously, the enhanced photocurrent for the nitrogen-doped $NaTaO_3$ photoanode can be attributed to the excited electrons from N 2p and oxygen vacancies local states.

In summary, we prepared well-dispersed and highly crystalline cubic $NaTaO_3$ particles and then doped nitrogen into the $NaTaO_3$ particles by thermal treatment in ammonia atmosphere.

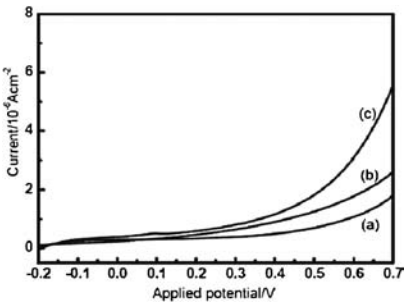

Figure 3. Photocurrent–applied potential curves of $NaTaO_3$ photoanodes on ITO substrate vs. Hg/HgCl reference electrode: (a) photoanode with the nitrogen-doped $NaTaO_3$ in dark, (b) photoanode with the undoped $NaTaO_3$, and (c) photoanode with the nitrogen-doped $NaTaO_3$ under the irradiation of visible light. Measurement condition: 0.1 M NaOH electrolyte solution, scan rate 5 $mV \cdot s^{-1}$. The illuminated photoanode surface was 1 cm^2.

The prepared nitrogen-doped $NaTaO_3$, compared to the undoped $NaTaO_3$, exhibits increased light absorption from 300 nm up to 550 nm. Correspondingly, the photocurrent density of the nitrogen-doped $NaTaO_3$ photoanode is enhanced under the irradiation of both UV–visible light and visible light.

The work was supported by Ministry of Science and Technology of China (No. 2009CB220001) and the Australian Research Council under its Centres of Excellence Program.

References and Notes

1 M. R. Hoffmann, S. T. Martin, W. Choi, D. W. Bahnemann, *Chem. Rev.* **1995**, *95*, 69.
2 A. Fujishima, X. Zhang, D. A. Tryk, *Int. J. Hydrogen Energy* **2007**, *32*, 2664.
3 I. Tsuji, H. Kato, H. Kobayashi, A. Kudo, *J. Am. Chem. Soc.* **2004**, *126*, 13406.
4 S. U. M. Khan, M. Al-Shahry, W. B. Ingler, *Science* **2002**, *297*, 2243.
5 W. Zhao, W. Ma, C. Chen, J. Zhao, Z. Shuai, *J. Am. Chem. Soc.* **2004**, *126*, 4782.
6 R. Asahi, T. Morikawa, T. Ohwaki, K. Aoki, Y. Taga, *Science* **2001**, *293*, 269.
7 G. Liu, Y. Zhao, C. Sun, F. Li, G. Q. Lu, H.-M. Cheng, *Angew. Chem., Int. Ed.* **2008**, *47*, 4516.
8 S. Sakthivel, M. Janczarek, H. Kisch, *J. Phys. Chem. B* **2004**, *108*, 19384.
9 C. Burda, Y. Lou, X. Chen, A. C. S. Samia, J. Stout, J. L. Gole, *Nano Lett.* **2003**, *3*, 1049.
10 S. Yin, H. Yamaki, M. Komatsu, Q. Zhang, J. Wang, Q. Tang, F. Saito, T. Sato, *J. Mater. Chem.* **2003**, *13*, 2996.
11 G. Liu, F. Li, Z. Chen, G. Q. Lu, H.-M. Cheng, *J. Solid State Chem.* **2006**, *179*, 331.
12 Y.-I. Kim, P. M. Woodward, K. Z. Baba-Kishi, C. W. Tai, *Chem. Mater.* **2004**, *16*, 1267.
13 M. Liu, W. You, Z. Lei, G. Zhou, J. Yang, G. Wu, G. Ma, G. Luan, T. Takata, M. Hara, K. Domen, C. Li, *Chem. Commun.* **2004**, 2192.
14 H. Kato, K. Asakura, A. Kudo, *J. Am. Chem. Soc.* **2003**, *125*, 3082.
15 Y. He, Y. Zhu, N. Wu, *J. Solid State Chem.* **2004**, *177*, 3868.
16 Y. Lee, T. Watanabe, T. Takata, M. Hara, M. Yoshimura, K. Domen, *Bull. Chem. Soc. Jpn.* **2007**, *80*, 423.
17 H. Kato, H. Kobayashi, A. Kudo, *J. Phys. Chem. B* **2002**, *106*, 12441.
18 K. Yang, Y. Dai, B. Huang, *J. Phys. Chem. C* **2007**, *111*, 12086.
19 N. Sakai, Y. Ebina, K. Takada, T. Sasaki, *J. Am. Chem. Soc.* **2004**, *126*, 5851.
20 I. Cesar, A. Kay, J. A. G. Martinez, M. Gratzel, *J. Am. Chem. Soc.* **2006**, *128*, 4582.
21 G. K. Mor, K. Shankar, M. Paulose, O. K. Varghese, C. A. Grimes, *Nano Lett.* **2005**, *5*, 191.
22 Supporting Information is available electronically on the CSJ-Journal Web site, http://www.csj.jp/journals/chem-lett/index.html.

Published on the web (Advance View) January 31, 2009; doi:10.1246/cl.2009.214